Analysis of rock lenses in extensional faults

Merethe Lindanger, Roy H. Gabrielsen & Alvar Braathen

Merethe Lindanger, Roy H. Gabrielsen & Alvar Braathen. Analysis of rock lenses in extensional faults. *Norwegian Journal of Geology,* vol. 87, pp. 361-372.Trondheim 2007. ISSN 029-196X.

Lenses in the cores of extensional faults represent a major uncertainty in fault seal predictions since they may influence flow paths in reservoirs. We investigate the dimensions of lenses in extensional faults, addressing 1) the position of the lenses relative to, or within, the fault core, 2) the influence of lithology, and 3) the mechanism active in the generation and development of the fault lens.
Rock lenses have been examined and measured in well-exposed extensional faults in three areas and in analogue experiments. The rocks hosting the lenses included in the study include nearly unconsolidated sandstone (Bornholm, Denmark), limestone interbedded with shales (Kilve, West England), and gneiss (Frøya, Central Norway). The remaining dataset is compiled from faults in analogue (plaster-of-Paris) experiments.
We determine the geometry of the lenses by normalizing length (measured in the dip-direction) and width (measured in the strike direction) to maximum thickness (c:a and b:a-ratios). It is found that several parameters affect lens shape: (i) Lithology affects the shape and the minimum/maximum sizes of the lenses, (ii) Primary (1st order) and secondary (2nd and higher orders) fault lenses commonly have different c:a-ratios, and finally, (iii) particularly for the most competent rocks, lenses in faults with several metres of vertical displacement tend to be relatively thicker than lenses occurring in faults with less displacement, probably reflecting a higher number of high order lenses in such zones.
The statistical average c:a-ratio for all lenses included in the study is 12,5:1.
Keywords: Fault architecture; fault geometry; fault-core lens

Merethe Lindanger: Department of Geoscience, University of Bergen, Norway, now at ResLab Integration AS, Kokstad, Norway. Roy H. Gabrielsen: Centre of Integrated Petroleum Research, (CIPR), University of Bergen, Norway, now at department of Geosciences, University of Oslo, Norway. Alvar Braathen: Centre of Integrated Petroleum Research, (CIPR), University of Bergen, Norway, now at the University Studies in Svalbard (UNIS), Norway.

Introduction

The internal architecture of faults and its related permeability structure are primary controlling factors on fluid flow in upper crustal, brittle fault zones (e.g. Wallace & Mearns 1986, Caine et al., 1996; Evans et al., 1997; Heynekamp et al., 1999). In cases where contacts between units of high or low permeability control the fluid flow across a fault, the fluid communication along the fault may be crucial for the bulk communication within the reservoir. This is particularly true when rock units which consist of stratified high- and low-permeable beds abut against the fault (Childs et al., 1997, Knipe, 1997; Knipe et al., 1997; Losh et al., 1999; Fredman et al., 2007, Færseth et al. 2007). In such cases, fluid flow within the fault zone itself may be of particular importance, because a permeable fault may contribute to the transport of fluids past the area covered by the non-permeable bed. Here, the geometry of fault lenses, their relative arrangement and their relation to intervening high-strain zones may be important for fluid communication along the fault. Still, internal fault architecture is rarely included in reservoir transmissibility evaluations (Manzochi et al., 1999, Caine et al., 1996), partly because of restricted calculation capacity for handling such complex geological structures. As the limitations caused by restricted capacity of numerical models are overcome, however, improved documentation of the geometry and dimensions of the internal structures of fault zones are necessary in the assessment of the total permeability of complex faults (e.g. Berg & Øian, 2007, Fredman et al. 2007 and references therein).

Different structural features contribute to defining the architecture of faults. These include the fault core where most of the displacement is accommodated, and the associated damage zones, which are commonly separated from the fault core by distinct fault-branches (Chester & Logan 1986, Gabrielsen & Koestler 1987, Schulz & Anders 1994, Caine et al., 1996, Færseth et al. 2007; Figure 1). The core of extensional, brittle faults frequently encompasses lozenge-shaped rock bodies, referred to as lenses or horses, which may occur in isolation, as *en echelon* trains, or be stacked to constitute duplexes (Gibbs, 1983; 1984, Gabrielsen & Koestler 1987, Gabrielsen & Clausen 2001, Clausen et al. 2003). The high-strain zones separating individual fault lenses or groups of such lenses may include deformed lithologies derived from the footwall- and hanging wall. Fault lenses are common elements in contractional faults (e.g. Boyer & Elliot, 1982, Davison 1994), strike-slip faults (e.g., Woodcock & Schubert, 1994) as well as in extensional faults (e.g. Gibbs, 1983; 1984, Gabrielsen & Clausen 2001, Lindanger et al. 2004, Childs et al. 1997). They are observed on all scales, from the seismic scale (Gibbs 1983, 1984), and down to cm and mm scales (e.g. Gabrielsen & Clausen, 2001, Clausen et al. 2003, Berg 2004, Christensen 2004). The lenses may consist of undeformed to heavily fractured host rocks (e.g., Koestler & Ehrmann, 1991; Childs et al., 1996), or be entirely dominated by fault rocks (Sibson 1977, Braathen et al. 2004).

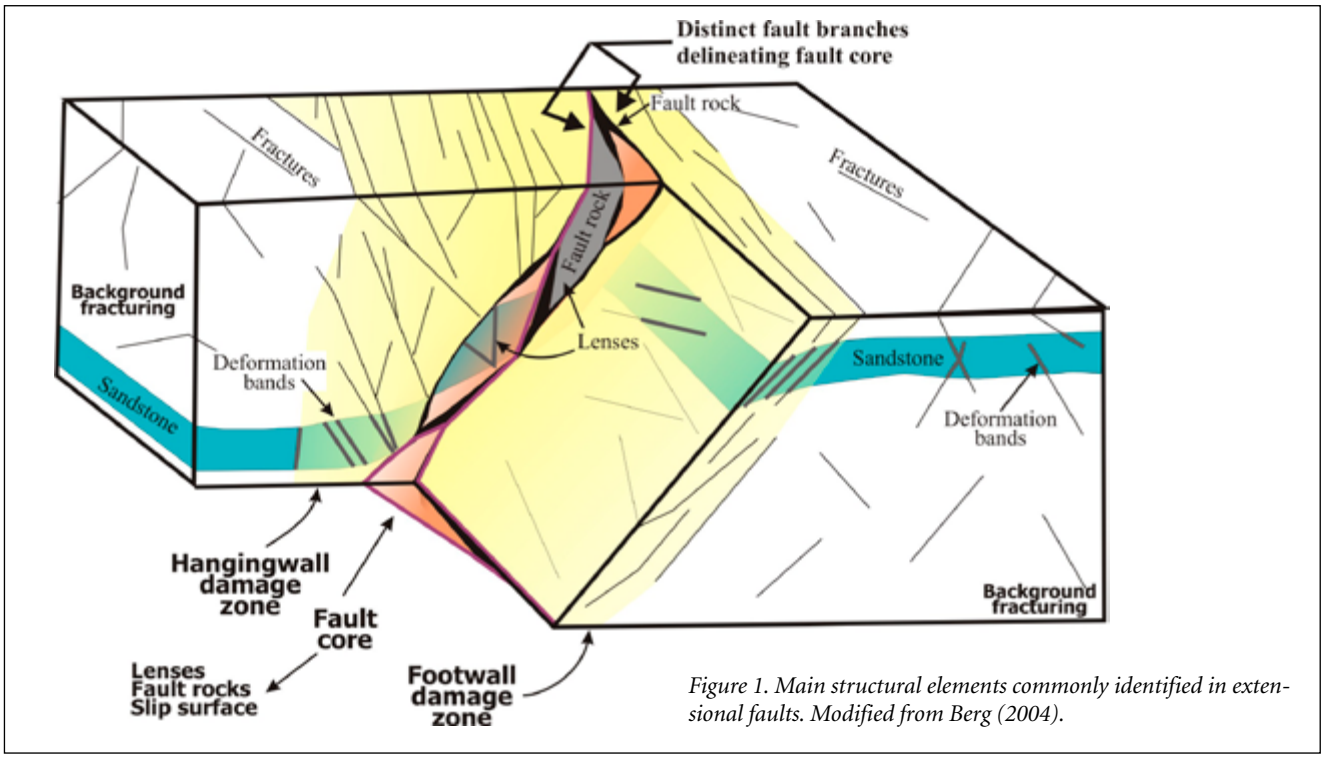

Figure 1. Main structural elements commonly identified in extensional faults. Modified from Berg (2004).

In this contribution we analyze the dimensions of fault-core lenses in extensional faults, using data from over 300 lenses. Our aim is not to establish robust statistical trends, but rather to investigate whether or not there are systematic scaling relationships for fault lenses that may be valuable in the establishment of fault geometry parameters to be included in reservoir models.

Data base and methods

In the present study, the length of the symmetry axes are used to estimate the geometry of the fault lenses. The axes are named according to their orientation in relation to the direction of tectonic transport and their orientation relative to the master fault (e.g. Ghosh 1993; Figure 2a). In the field, this approach has some methodological constraints because lenses are rarely exposed in full and because the sections available sometimes are at oblique angles to the ideal. Care has therefore been taken to find and document lenses that are fully exposed. When only parts were exposed only those sections situated closest to the central part of the lens were selected for study. Measurements were included in the database only in the cases where the lens was seen to decrease in thickness away from its central area in both directions along the axis measured. In cases where the maximum thickness (t=a; Figure 2a) is measurable and the tip line of the lens in the direction of one of the main axes is observed, simple calculations are sufficient to establish the relative dimension of the lens. Our studies indicate that lenses are generally symmetric or nearly symmetric (see also Clausen et al. 2003). This principle is particularly useful in cases where it is not certain that the maximum axes are exposed, so

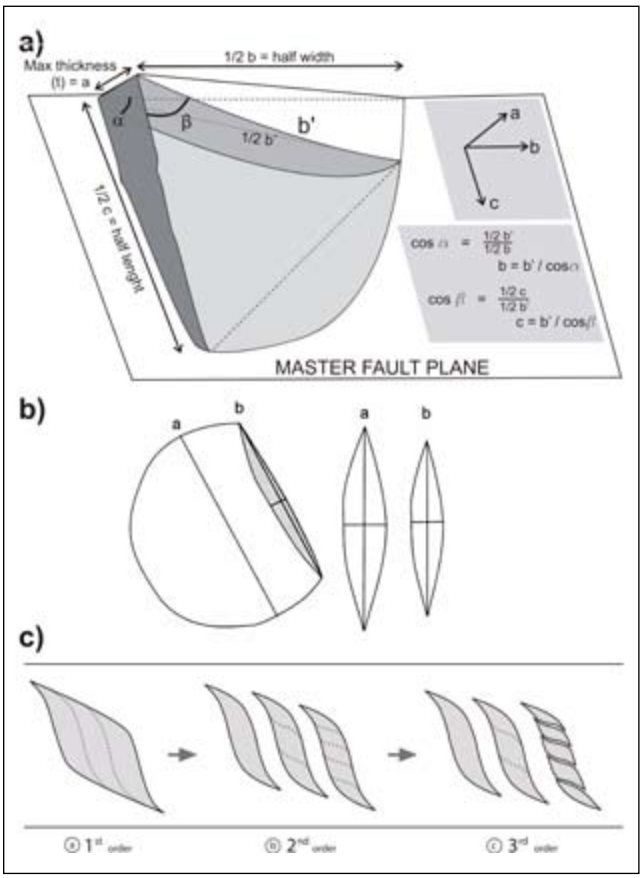

Figure 2. a) Fault lens with kinematic axes and dimensions as measured in the field. Calculation of a-axis and b-axis from observed section (shaded in grey) is indicated. b) Because of the symmetry of the lenses, the c:a ratio (dip:thickness-axes ratio) is robust even in cases where the entire lens is not available for measurement. c) Progressive break-down of lenses produces lenses of different "orders".

that the measured axis is a minimum value only. Assuming a regular symmetry of the lens, this is a minor problem, because the ratios between the axes are constant when parallel sections are considered (Figure 2b).

In some cases, it is clear that one larger lens is preserved at the stage of being cut into several smaller lenses. Here, the original lens is classified as a *first-order* lens and the smaller lenses are termed *second-order* lenses. It follows that deformation may further split the second-order lenses into third- and fourth-order lenses, and so on (Figure 2c). Particular emphasis was put on identification of the different orders (1st, 2nd, 3rd) of the lenses in the context of their initiation, further development and position within the fault core. Furthermore, the width of the fault core and the amount of displacement across the fault were recorded.

Altogether, the longest, intermediate and shortest axes of 323 rock lenses from 12 separate faults have been recorded. The host rocks of the faults investigated in this study include migmatitic gneiss (Island of Frøya, Mid-Norway), limestone interbedded with shale (Somerset, England) and nearly unconsolidated sandstone with mudstone layers (Bornholm, Denmark). In addition, data from analogue, mechanical experiments using plaster-of-Paris, performed and previously analyzed by Gabrielsen & Clausen (2001) were included. It is emphasized that the conditions for deformation were less brittle in the plaster-of-Paris experiments than in all the other faults included in the study.

Study areas and experiments

Faults in sedimentary rocks (two areas) and metamorphic rocks (one area) were selected such that their throws range over four orders of magnitude, from Cm's to tens of meters. The recordings from cm-scale structures were mainly done at one locality on Bornholm and on the analogue plaster-of-Paris experiments, but structures at this scale were also occasionally found at the other sites studied. Furthermore, the experiments were used to obtain additional information on the dynamics of the generation of fault-core lenses (see Gabrielsen & Clausen 2001).

At the first study site (Faults I and II; the island of Frøya, central Norway; Figure 3), the rocks are quartzofeldspatic migmatitic gneisses intruded by granite/tonalite and affected by faults that truncate the metamorphic foliation. The rock fabrics are Late Palaeozoic (Caledonian), but also multistage late- to post-Caledonian fault reactivation (Devonian – Tertiary) is documented in the nearby Møre-Trøndelag Fault Complex (Blystad et al., 1995; Grønlie & Roberts 1989, Gabrielsen et al., 1999; Osmundsen et al. 2006). A similar development is assumed for the other faults of the region (Olsen et al. 2007, Redfield et al. 2007). Two road sections on Frøya were studied: In Fault I (Flatval), lenses are located within the fault core of a nearly vertical, dominantly dip-slip fault with slight indications of strike-slip reactivation. Fault II (Skardsvåg) is an extensional normal fault dipping approximately 80° to the southeast and with a vertical separation of approximately 5 meters (Eliassen 2003; Figure 4a-c). Lenses of four different orders were identified at this locality.

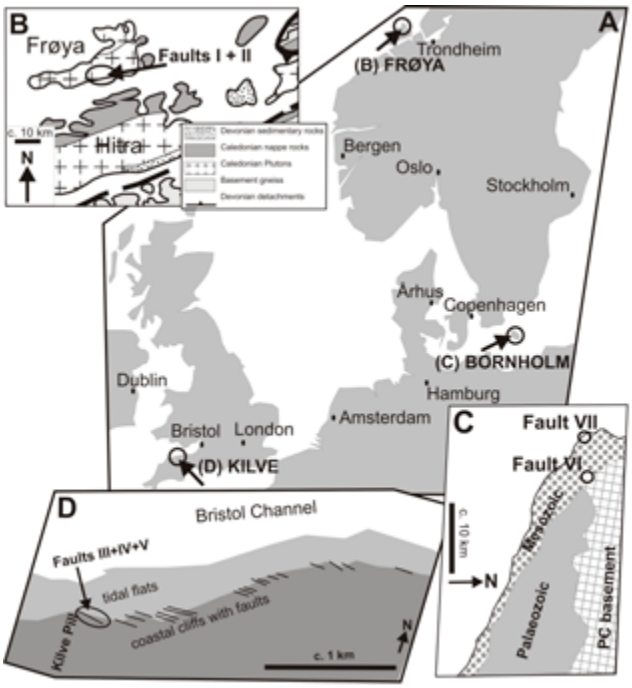

Figure 3. A) Location map for study areas; B) Frøya, C) Bornholm, and D) Kilve.

The site on Kilve Beach is situated on the southern margin of the Bristol Channel Basin, England (Figure 3). This basin forms part of a series of Mesozoic extensional grabens in southern England which have experienced slight inversion in Tertiary times (e.g., Whittaker & Green, 1983; Loyd et al., 1973; Kamerling, 1979; Chadwick, 1986). The host rocks are argillaceous limestones interbedded with organic-rich claystone. The three faults studied (Faults III, IV and V) have normal separation between 4 and 19 meters. The study area was carefully scrutinized to avoid structures affected by inversion. Hence, no indications of inversion are seen in faults included in this study. Faults III and IV represent the same master fault (or two closely spaced branches of this fault) exposed in two different cliff sections, approximately 40 meters apart. In both exposures, the lenses occur both centrally in the fault core and along the borders towards the damage zones (Figure 5a-c). The fault cores display lenses of particularly competent limestone in addition to subordinate limestone breccia and shale gouge. The lenses are separated from the damage zone by distinguishable fault branches, whereas the primary stratification can be identified throughout the damage zones. Fault V is exposed on the beach, revealing the strike dimension (b-axes) of the lenses. Both limestone breccia and shale gouge are present within the fault core. The lenses consist either entirely of shale or of limestone. However, the major-

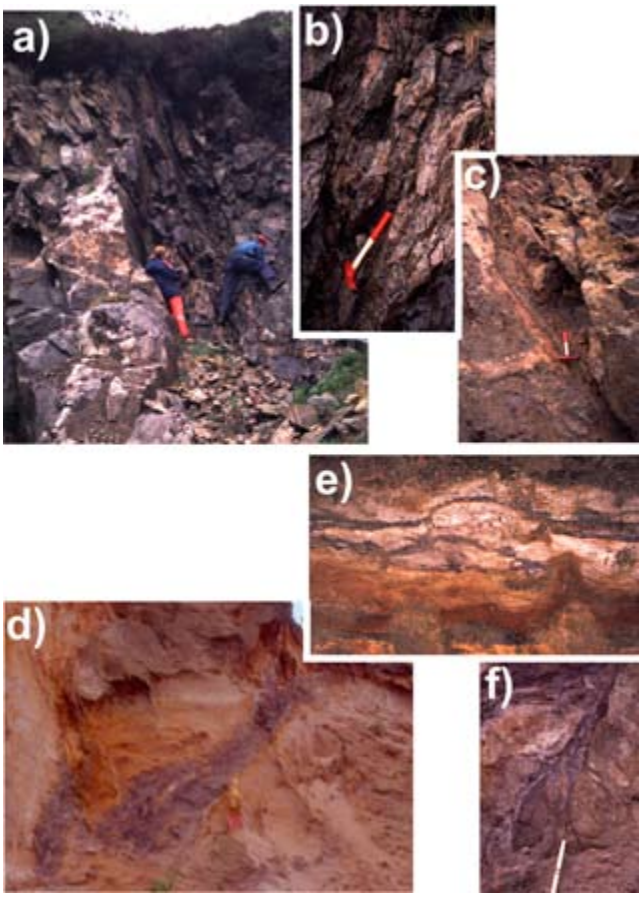

Figure 4. Fault core lenses from Fault I (a and b) and Fault II (c) in gneiss, island of Frøya, and fault core lenses from Fault VI in poorly consolidated sandstone, Bornholm (d-f). See text for description.

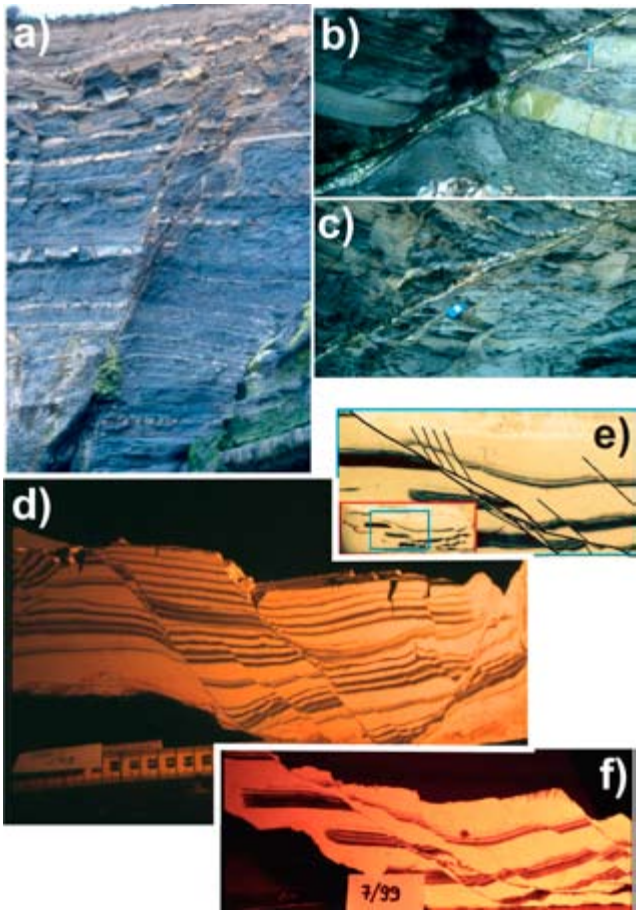

Figure 5. Array of fault core lenses (a) and details from Faults II and IV (b and c) in interbedded limestone and mudstone, Kilve Beach, Bristol Channel and Faults XIII, IX and X from analogue plaster-of Paris experiments (d-f). See text for description.

ity of the lenses are made up of limestone and shale bed fragments in which primary bedding can easily be recognized.

The study area on Bornholm (Figure 3), Denmark reveals extensional faults that are hosted by poorly consolidated fine-grained sand and silt, interbedded with layers of clay belonging to the Lower Cretaceous Robbedal Formation of the Nyker Group (Gravesen et al. 1982, Liboriussen et al. 1987). The rocks have experienced a maximum burial of ca. 500 m (Hamann 1988). Minor inversion (Late Cretaceous – Early Tertiary; Vejbæk et al., 1994) has been described from the area, but was not detectable in the faults studied by us. Two sites were studied. Fault VI is within a sand pit (A. Stenders Kvartsgrav) and has an overall normal separation of a minimum of 13 m (Clausen et al., 2003). Lenses are present within the fault cores in four out of six fault branches (Figure 4d-f). The lenses consist of medium to coarse-grained sand bodies separated by clay membranes. Faults VIIa-d are found within a cliff section (Galgeløkken Cliff) on the beach south of the town of Rønne. These are normal faults with vertical throws of only 0.4 - 4.5 cm and contain small, isolated lenses. The sediments here are heterolithic sands and muds of the Lower Jurassic Rønne Formation of the Bornholm Group, which have had a maximum burial of 1200 m (Hamann 1988). The fault lenses consist of fine-grained sand draped by thin laminae/layers of clay. Due to the poor consolidation of the rocks on Bornholm, it was possible to obtain very good strike- and dip-sections of the lenses by excavation (Clausen et al. 2003).

Data on lenses in plaster-of-Paris were obtained from five experiments (Faults VIII – XII, Figure 5d-f). The plaster represents by far the mechanically weakest material included in this study. A description of the experimental set-up and the methodological constraints for this type of experiment is given by Fossen & Gabrielsen (1996) and Gabrielsen & Clausen (2001). This data set, which is based on the experiments performed by Gabrielsen and Clausen (2001), who did not analyze the dimension of the fault lenses, consists of measurements of dip-dimensions and thicknesses, but some lenses were also measured in the strike dimension by studying the geometry on the top surface. Vertical displacements of the faults vary between 1 and 10 cm. Since the sequential development and growth of the lenses are known, the mechanisms involved in their origin can be established. In the experiments performed by Gabrielsen & Clausen (2001), the majority of the fault lenses resulted either from segment splaying, segment amalgamation or by asperity bifurcation (see explanations in Figure 6).

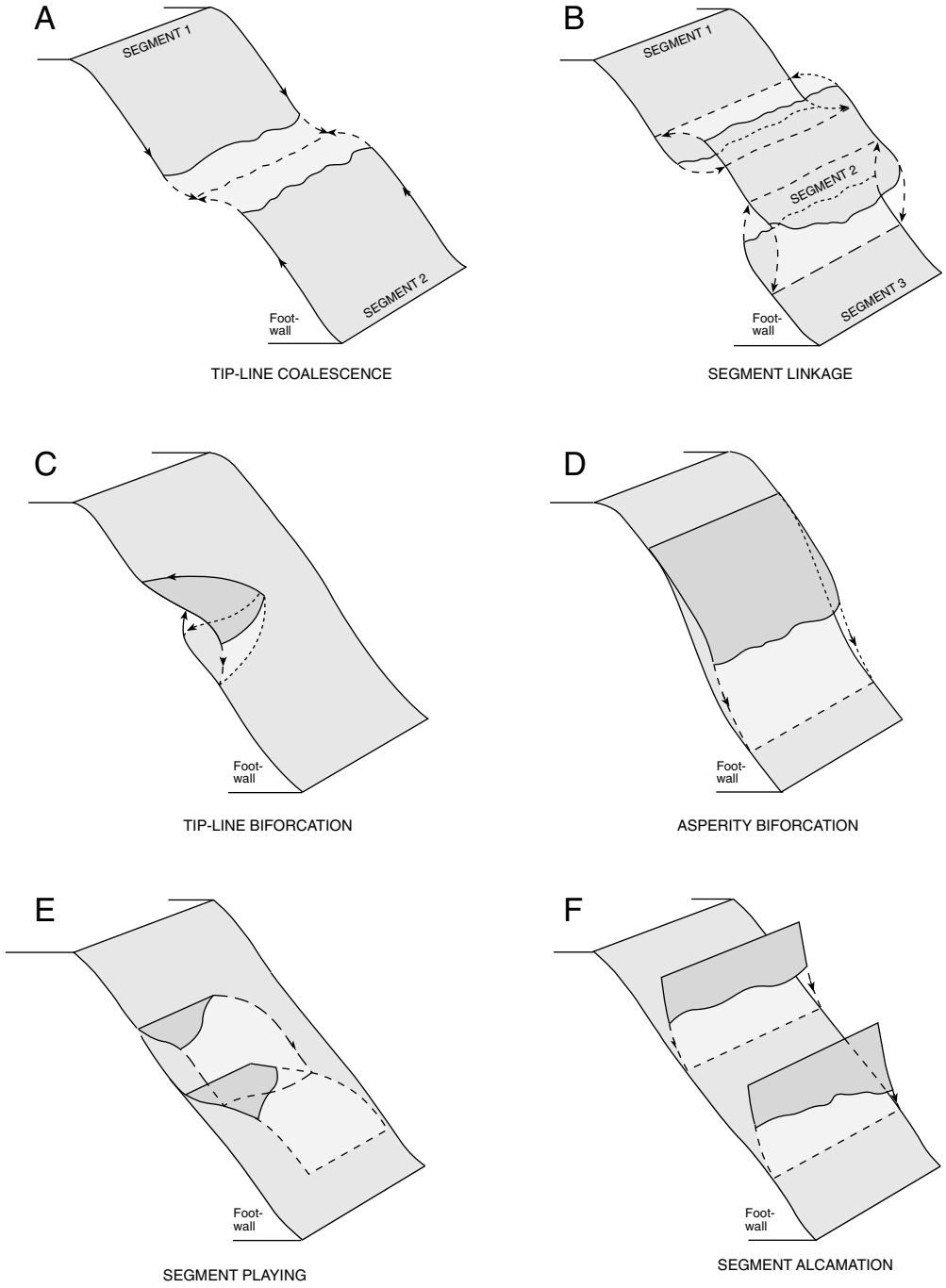

Figure 6.
Principal configurations of fault segments during development of fault lenses.
(a) Tip-line coalescence, (b) segment linkage, (c) tip-line bifurcation (d) asperity bifurcation, (e) hanging-wall segment splaying,
(f) hanging-wall segment amalgamation. The most common mechanisms observed in the present data are segment linkage and asperity bifurcation. Modified from Gabrielsen & Clausen (2001).

Dimensions of fault-hosted lenses

Length(dip)–thickness relations of all recorded fault lenses are presented in Figure 7e. More specifically, Figure 7a shows data for lenses hosted by faults in migmatitic gneiss (Frøya). This is the rock with the greatest mechanical strength among those included here. The average c:a-ratio for the entire population is 17:1 (Table 1). In greater detail, the lenses in the core of Fault I vary between 4 and 26 cm in thickness and between 52 and 170 cm in length. The average c:a-ratio for Fault I is 8:1. The thicknesses of the lenses in Fault II are between 3 and 22 cm, the lengths vary between 21 and 300 cm with an average c:a-ratio of 20:1.

For comparison, the dip-length axes (c-axes) of the lenses in cores of faults studied at Kilve Beach are

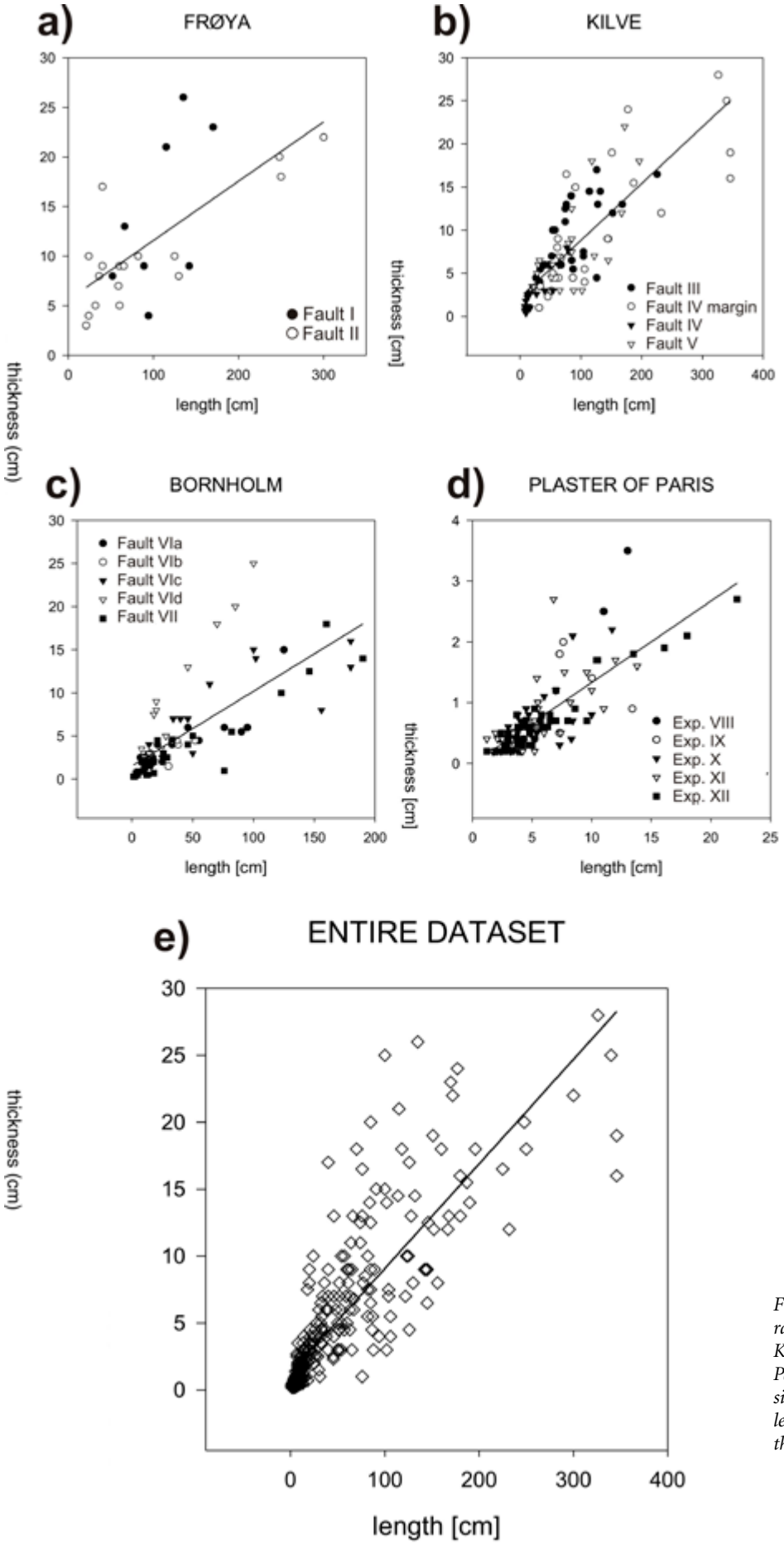

Figure 7. Plot of length versus thickness-ratio (c:a) of the lenses on (a) Frøya, (b) Kilve, (c) Bornholm and (d) plaster-of-Paris analogue experiments. The regression line in each plot represents all the lenses for that specific area. (e) Plot of the complete data set. See also Table 1.

Dataset	N	Regression analysis (a = Nc + M)	R^2 confidence	Relative Length (c) vs width (a) ratio
Frøya, all lenses	25	a = 0,06c + 5,60	0,47	16,7:1
Frøya, fault I	8	a = 0,12c + 0,93	0,36	8,3:1
Frøya, fault II	17	a = 0,05c + 5,32	0,67	20,0:1
Kilve, all lenses	96	a = 0,06c + 2,42	0,65	16,7:1
Kilve, fault Iii	27	a = 0,04c + 4,27	0,54	22,2:1
Kilve, fault IV transition zone	27	a = 0,06c + 2,49	0,66	16,7:1
Kilve, fault IV fault core	21	a = 0,09c + 0,37	0,78	11,1:1
Kilve, fault V	21	a = 0,08c + 1,70	0,51	12,5:1
Bornholm, all lenses	83	a = 0,09c + 1,523	0,57	12,5:1
Bornholm, fault VI	53	a = 0,05c + 3,73	0,20	20,0:1
Bornholm, fault VIa	13	a = 0,08c + 1,31	0,72	12,5:1
Bornholm, fault VIb	5	a = 3,53c + 24,59	0,30	0,28:1
Bornholm, fault VIc	22	a = 0,08c + 1,69	0,74	12,5:1
Bornholm, fault VId	13	a = 0,24c + 0,98	0,93	4,2:1
Bornholm, fault VII	30	a = 0,08c + 0,43	0,87	12,5:1
Plaster-of-Paris, all lenses	119	a = 0,13c - 0,01	0,59	7,7:1
Plaster-of Paris, exp. VIII	7	a = 0,30c - 0,58	0,97	3,3:1
Plaster-of Paris, exp. IX	10	a = 0,09c + 0,30	0,20	11,1:1
Plaster-of Paris, exp. X	27	a = 0,13c - 0,00	0,44	7,7:1
Plaster-of Paris, exp. XI	33	a = 0,13c + 0,06	0,47	7,7:1
Plaster-of Paris, exp. XII	42	a = 0,12c - 0,03	0,88	8,3:1
Complete dataset	323	a = 0,08c + 1,26	0,71	12,5:1

Table 1. Fault data on lenses, including the number of lenses studied, linear regression lines for various parts of the dataset, R^2 confidence factor for the regression lines, and the length (c-axis) versus width (a-axis) relationship. The latter relationship calculates as c/a = 1/N. Note that all data except the row presenting all lenses from Kilve give best fit to linear regression lines. The Kilve dataset has a best fit for a power trend ($a = 0{,}18c^{0{,}83}$; $R^2 = 0{,}74$).

between 8 and 346 cm and the thickness between 0.4 and 28 cm (Figure 7b). The average c:a-ratio is 14:1, which implies that the lenses on average are thinner compared to those examined in Fault I on Frøya. When only the lenses in Fault III are considered, the c:a ratio is 22:1, whereas the equivalent ratios for faults IV and V are 11:1 and 13:1, respectively. The fault core lenses along the margin of fault IV have an average length-thickness (c:a) ratio of 17:1. It is noted that these incipient lenses in the transition zone to the damage zone are almost identical to those of the other faults (ratio of 14:1).

The lenses examined in the nearly unconsolidated, sand and clay units on Bornholm are presented in Figure 7c (Faults VI and VII). The lengths of these lenses vary between 1.3 cm and 190 cm and the thicknesses between 0.3 cm and 25 cm. The average c:a-ratio for all data from the Bornholm faults is 13:1. When only Fault VI, which has an accumulated displacement of approximately 13 m is considered, the average c:a ratio is higher (20:1). For Fault VII, with a dip-slip-separation of cm, the ratio is 13:1, indicating that in the poorly consolidated sandstone, faults with only minor displacement have lenses that are thicker than those with greater displacements..
The diagram in Figure 7d shows the lenses examined in the plaster-of-Paris experiments. Here, the lengths vary between 1.2 and 22.2 cm and the thicknesses between 0.2 and 3.5 cm. The average c:a ratio is 8:1.

By combining all the data (Figure 7e), lenses in this study have lengths between 1.2 cm and 346 cm and thicknesses between 0.2 and 28 cm. The absolutely smallest c:a-ratio for the lenses is 3:1, which is the ratio for a lens measured in experiment VIII (plaster-of-Paris). In contrast, the largest c:a ratio (22:1) is the ratio for a lens in fault III in Kilve. The average lens (all data) has a c:a ratio of 12,5:1, with a correlation coefficient (R^2 confidence) of 0,71. The average of 12,5:1 is therefore considered to be statistically robust for the faults included in the present study.

Analysis and discussion

Several factors are likely to influence the development and geometry of fault core lenses. These include tectonic setting and orientation of the principal fault plane, lithology of the host rock, bulk fault displacement, magnitude of the principal stresses and the dominant mechanism operative in the generation and development of

the lenses. Also, dynamic processes like change in fluid pressure and temperature and strain-hardening and strain-softening are of significance. The present study includes only normal (extensional) faults. The fault dips are of similar magnitude (40 – 80°), with one exception, Fault I at the Frøya locality which is more steeply dipping. Hence, the orientation of the principal stress axes was similar for the faults included in the study.

The present data have mainly been collected to constrain the general geometry of fault lenses, and this allows for the relation between initiation mechanism and geometry of the lenses to be addressed only to a limited degree. Nevertheless, observations have been made that can be used in the evaluation of the mechanism for first-order fault lens generation, as well as for the further segmentation of the lenses in some cases. When studying the shapes of the lenses (b:a and c:a ratios) in order to correlate these with the deformation mechanism, it is crucial first of all to include only cases where the interrelation between the lenses can be clearly determined (Figure 2c) and secondly, to distinguish mechanisms that are related to the primary initiation of the lenses from secondary mechanisms that are associated with the collapse of the lenses by continued strain. A certain identification of the mechanism responsible for lens initiation can only be made for cases where the lens has not been transported away from the part of the fault from which it was derived.

Lens geometry and the lithology of the host rock

Table 1 and Figure 8 summarize the average c:a ratios of fault core lenses from the faults I-XII. This value varies between 3:1 (Experiment VIII, plaster-of-Paris) and 22:1 (limestone, Kilve). It is noteworthy that the average c:a-ratio for the lenses in gneiss (Faults I and II at Frøya) is 17:1, which lies between the values obtained from poorly consolidated sandstone and limestone. Systematic differences in c:a ratios observed for faults in different lithologies are illustrated in Figure 9. In a log-log-plot (Figure 9A) the fault lenses derived from different rock types display nearly similar trends for those with c-axes longer than 10 cm. For smaller values of c, the trends of the curves suggest that there are contrasting minimum values for the a-axes (thickness) for lenses derived from different rock types, so that the thickest lenses derive from the mechanically most competent lithologies (see also Figure 8B). In this context, the results from the plaster-of-Paris experiments fall in a special category, having very low minimum values. This is to be expected, since the plaster-of-Paris experiments were conducted under conditions near the ductile-brittle transition and also because of the very fine-grained and homogeneous nature of this material. In a linear plot (Figure 9B), showing the absolute c:a ratios, and covering the range between 0 and 100 cm, the contrasts between the lithologies are even clearer. The lenses derived from gneisses are characterized by the higher c:a ratio within the window of observation, compared to that of the weaker sediments. The gradients of the regression lines are rather similar, although it

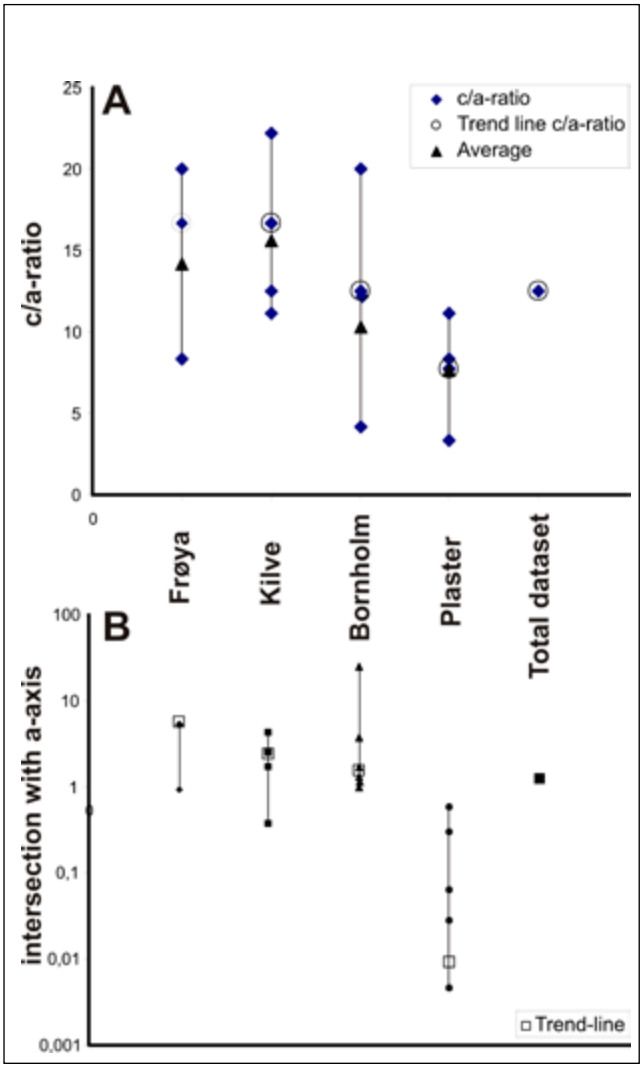

Figure 8. Plot of datasets from Frøya, Kilve, Bornholm, plaster-of-Paris, and the total dataset, addressing; (A) Range of c:a-ratios, including the average c:a-ratio and the trend line c:a-ratio for each site; (B) Intersection with a-axis plotted on logarithmic scale for each fault studied and the intersection for the summary trend line for each site (N-numbers in table 1).

is notable that the weaker lithology (poorly consolidated sandstone) has a slightly steeper gradient in the diagram. However this difference is not considered statistically significant. This diagram also displays a cut-off value, which decreases with decreasing mechanical strength, indicating that full collapse of the lenses and degradation into fault rocks occurs at different stages of deformation for different lithologies.

Development and splitting of fault lenses

Previous studies have shown that several mechanisms (tip-line coalescence, segment-linkage, asperity bifurcation, splitting by internal shear; Peacock & Sanderson 1991, Childs et al. 1996, 1997, Gabrielsen & Clausen 2001) are active in the initiation and further development of fault-core lenses (Figure 6). In the study of such relations, the plaster-of-Paris-experiments have proven

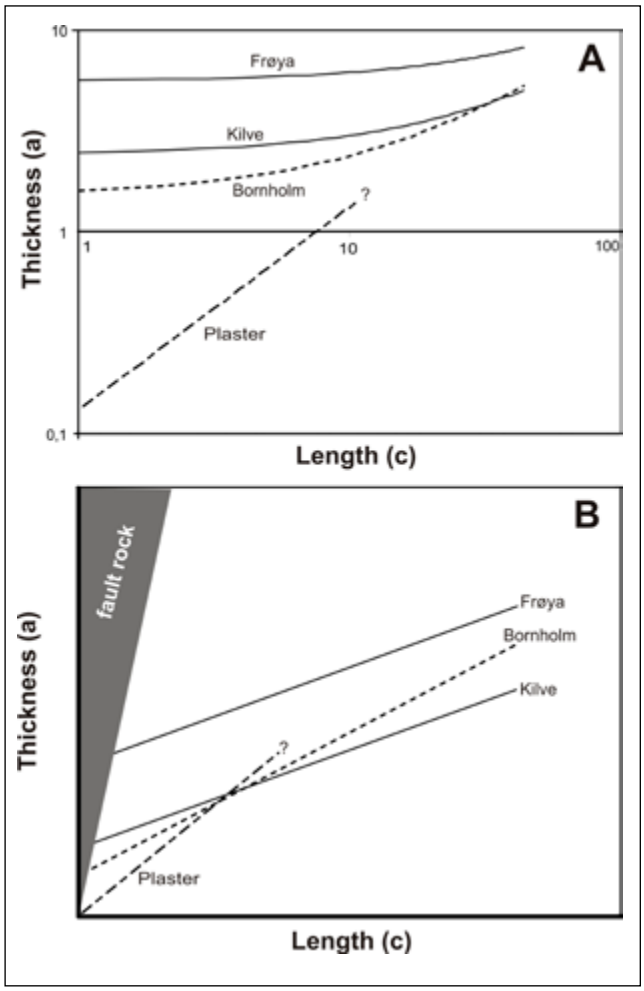

Figure 9. (A) Linear regression lines for the datasets of the four locations/lithologies studied, presented in log-log plot on cm scale (see Table 1). Note that the lines curve towards different intercepts for thickness, indicating that the relatively stronger rocks at Kilve (limestone) and Frøya (gneiss) have a larger minimum lens thickness. (B) Plot of relative relationship between length and thickness (window of 0-100 cm) for lenses of Frøya, Kilve, Bornholm, and plaster-of-Paris, based on established linear trend lines. Relatively weak rocks intercept at very low values, suggesting they can form small lenses, whereas gneiss and limestone break down to fault rock before reaching this level.

particularly valuable (Gabrielsen & Clausen 2001, Lindanger et al. 2004), suggesting that asperity bifurcation (lenses being derived from uneven or curved segments of the footwall or hanging wall) is the most common mechanism for fault-lens initiation. Examples of lenses, which are most likely derived by this mechanism, are observed at several of the localities included in this study (e.g. Figures 4c, 5a and c).

Another mechanism for fault-lens initiation involves the interaction of Riedel shears and other secondary fractures. Since rock strength influences the orientation of the plane of shear failure, according to Coulomb's theory, this implies that the initial angle (relative to the master fault) of Riedel shears depends on the mechanical strength of the host rock (Figure 2c). This, as can be expected, should cause differences in the geometry of the fault lenses (e.g. Wojtal 1994), an effect that would be particularly evident in layered rocks where the beds have contrasting mechanical strength (Peacock & Sanderson, 1991; Rykkelid & Fossen 2002, Berg 2004), producing lenses of variable geometry (e.g. Figures 5a and b).

The present study confirms that fault lenses may become split into sub-lenses of higher order by continued strain (2nd, 3rd and 4th order; Figure 2c). Although it cannot be established how common the different mechanisms are for the generation of first order and subsequent generations of lenses, the spatial relationship between, and the relative geometry of, different orders of lenses can still be studied in some of the faults included in this study. It should be noted that the mechanism responsible for lens initiation can be determined only in cases where the lens has been transported a short distance, so that it has not completely lost contact with its point of origin. Although there is not sufficient data to analyse the initial lens-forming mechanism in greater detail, some observations regarding the break-down of lenses have been made.

In Fault I on Frøya, 3rd-order lenses are framed by 4th order lenses (Figure 10a). The average c:a-ratio for the third-order lenses is 13:1 compared to 7:1 for the fourth-order lenses. A similar relationship is found for Fault V (Kilve) where a second-order lens is seen to break down into third-order lenses (Figure 10b). Here the 2nd-order lens has a c:a ratio of 18:1, whereas the c:a ratio for the 3rd-order lenses is 15:1. More examples with similar relations are found in Fault VIIa (Figure 10c) and Fault VIIe (Figure 10d) on Bornholm.

In summary, there is a tendency for high-order fault lenses in the most competent rocks to have a lower c:a ratio, so that 2nd-order lenses tend to be relatively speaking thicker than 1st-order lenses. The most obvious explanation for this is that lenses are initiated by Riedel shears cutting through the pre-existing lens at a typical angle of approximately 30° or less (Anderson, 1951; Wojtal, 1994; Peacock & Sanderson, 1992). This implies that higher-order lenses developed in competent lithologies, such as gneiss, disintegrate into relatively thicker lenses whereas lenses in basically unconsolidated sandstone split into thinner ones. Exceptions to this rule are seen in some faults at Kilve, for example, in Fault VIIa, where five 2nd-order lenses make up one 1st-order lens. Here the c:a ratio for the first-order lens is 8:1, whereas it is 11:1 for the 2nd-order lenses. The extremely thin nature of some of the lenses in this fault suggests that other mechanisms than splitting of the lower order fault lenses dominated.

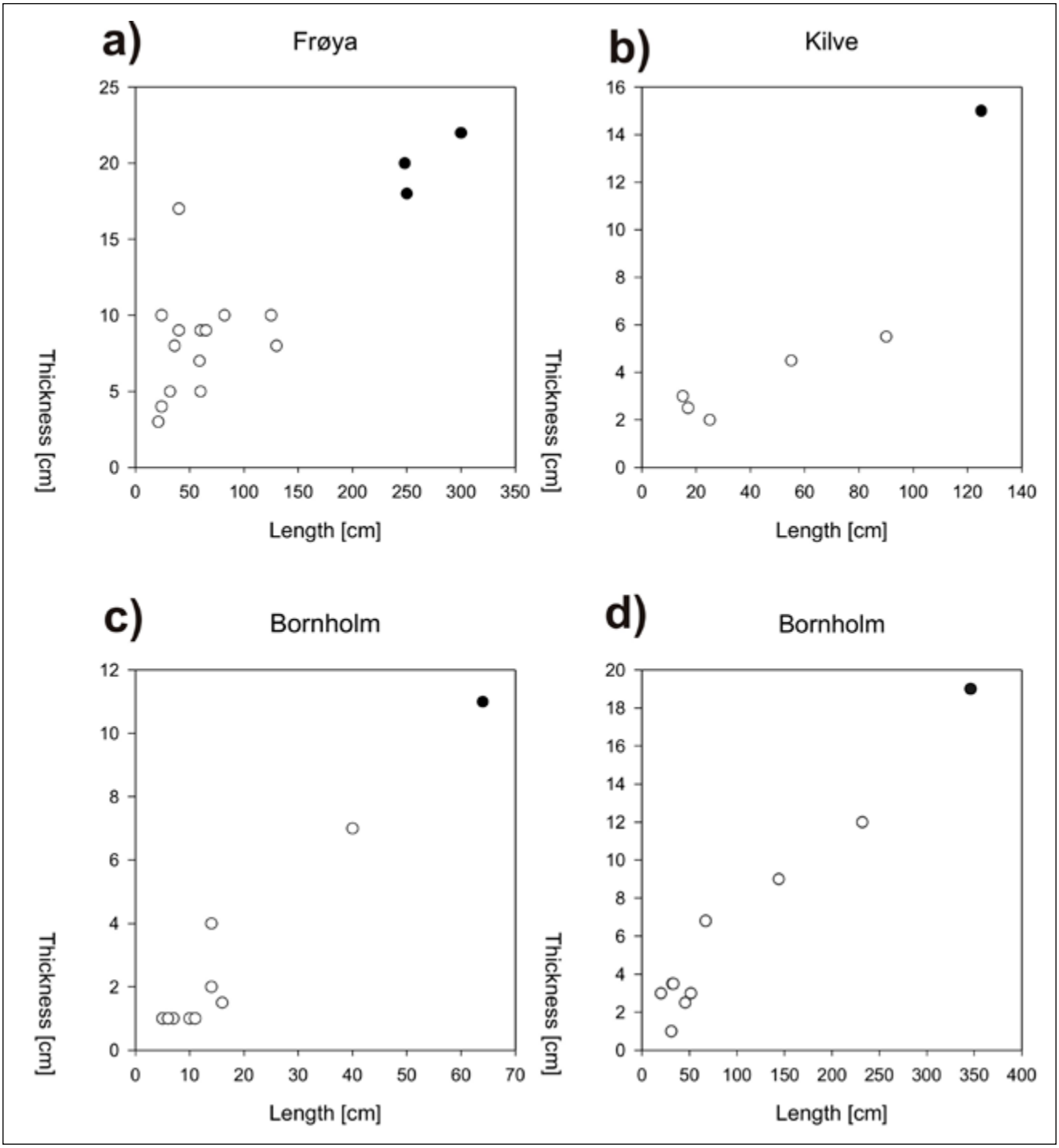

Figure 10. Plots of c:a-ratios for lower-order (filled circles) and subsequent higher-order lenses (open circles) from selected faults. (a) Fault I, Frøya; (b) Fault V, Kilve; (c) Fault VIIa, Bornholm; and (d) Fault VIId, Bornholm.

Summary and conclusions

Field observations and analogue mechanical experiments suggest that the development of fault core lenses is a highly dynamic process, the mechanisms of which are likely to change from the primary (initial) to the more advanced stages of shear (secondary). Thus, it is important to distinguish between the lens-forming mechanisms at different stages of development. The present study has been performed to study the variation of geometrical relations in fault lenses, and has to a lesser degree focused on the primary mechanisms behind fault lens generation. The variance in the geometry of fault lenses is generally systematic and suggests that lenses that developed in interbedded argillaceous limestone and shale and poorly consolidated sandstone are thinner than those developed in gneiss, which is to be expected if primary shear fractures are deflected at a more obtuse angle to the master

fault in the mechanically stronger layers.

The present study suggests that the average fault lens geometry changes and sometimes becomes more varied as deformation progresses. The reason for the changing average geometry of lenses is the combined initiation of new (1st order) ones and the break-up and decay of those that were already generated, into new lenses (2nd and higher orders). In many cases, the splitting of 1st order lenses into 2nd order ones seems to take place by the development of new fractures in the direction of maximum shear (Riedel shears) and results in shorter and, relatively speaking, thicker lenses.

The great majority of the fault lenses investigated in the present study have c:a ratios between 1:9 and 1:15. This includes data from rocks of a relatively wide range of lithologies. When all the fault lenses measured in this study are included in the regression analysis, an average linear c:a ratio of 12,5:1 is obtained. Lenses in faults with a large vertical displacement seem to be relatively thicker than those in faults with lesser displacement. This may again be related to the specific mechanism active during their generation, as lenses generated in late stages of faulting seem to be primarily generated by coalescence of Riedel shears and other secondary fractures, whereas segment splaying and amalgamation seem to be the dominating mechanism of lens development in earlier stages.

The present study is a first attempt to determine general limits for the dimensions of fault core lenses in extensional faults. It also relates the geometries to the total displacement across the fault and the stage of development of the lenses in faults with moderate displacements (less than a few tens of meters). The study includes data from lithologies with contrasting mechanical strength. It is suggested that there are some general ratios for the geometry of fault lenses. However, it is necessary to extend the database to include more faults in different lithologies and to study in more detail the process of splitting and decay of fault lenses and their associated geometries, before lens shapes and the mechanism for the formation of different generations of lenses can be said to be fully explored.

Acknowledgements: This study was initiated under the "Oil recovery in fractured reservoirs" program and carried out within the Centre of Integrated Petroleum Research (CIPR), both supported by the Norwegian Research Council as a Strategic University Program (SUP) and a Centre of Excellence, respectively. The paper has benefited from numerous discussions in the field and the laboratory with Silje Støren Berg, Jill A. Clausen, Håkon Eliassen, Rune Kyrkjebø and Tore Skar and also from critical remarks and useful suggestions by two anonymous referees. Figure 2 was drafted by Randi Bäckmark.

References

Anderson, E. M. 1951: *The dynamics of faulting and dyke formation with application to Britain.* Oliver & Boyd (eds.), 209 pp.

Berg,S.S., 2004: *The architecture of normal fault zones in sedimentary rocks: Analysis of fault composition, damage zone asymmetry, and multi-phase flow properties.* PhD-thesis, University of Bergen, 118 pp.

Berg, S. S., Skar, T., Braathen, A. & Gabrielsen, R. H., in press. Internal fault core characteristics of normal faults: Outcrop analyses from the Somerset Coast and SE Utah. *Journal of Structural Geology.*

Berg S.S. & Øian, E., 2007: Hierarcical approach for simulating fluid flow in normal fault zones. *Petroleum Geoscience 13*, 25-35.

Blystad, P., Brekke, H., Færseth, R. B., Larsen, B. T., Skogseid, J. & Tørudbakken, B. 1995: Structural elements of the Norwegian continental shelf. Part II: The Norwegian Sea Region. *Norwegian Petroleum Directorate Bulletin 8*, 45 pp.

Boyer, S. E. & Elliot, D., 1982: Thrust systems. *American Association of Petroleum Geologist Bulletin 66,* 1196-1230.

Braathen, A., Osmundsen, P.T. & Gabrielsen, R.H., 2004: Dynamic development of fault rocks in a crustal-scale detachment: An example from western Norway. *Tectonics 21.* TC4010, 1-21.

Caine, J. S., James, P. E. & Forster, G. B., 1996: Fault zone architecture and permeability structure. *Geology 24* (11), 1025-1028.

Chadwick, R. A., 1986: Extension tectonics in the Wessex Basin, southern England. *Journal of the Geological Society, London 143,* 465-488.

Chester,F.M. & Logan,J.M.,1986: Implications of mechanical properties of brittle faults from observations of the Punchbowl fault zone, California. *Pure and Applied Geophysics 124*, 77-106.

Childs, A. D., Nicol, A., Walsh, J. J. & Watterson, J., 1996:. Growth of vertically segmented normal faults. *Journal of Structural Geology 18,* 1389-1398.

Childs, C., Walsh, J. J. & Watterson, J., 1997: Complexity in fault zone structure and implications for fault seal prediction. *In:* Møller-Pedersen, P. & Koestler, A. G. (eds.), Hydrocarbon Seals: Importance for Exploration and Production. *Norwegian Petroleum Society (NPF) Special Publications 7*, 61-72.

Christensen, M., 2004: *Soft sediment faulting – Investigation of the 3D geometry and fault zone properties.* Ph.D-thesis, University of Aarhus, 146 pp.

Clausen, J. A., Gabrielsen, R. H. & Johnsen, E., 2003: Fault architecture and clay smear distribution. Examples from field studies and drained ring-shear experiments. *Norwegian Journal of Geology 83* (2), 131-146.

Davison, I., 1994: Linked fault systems; extensional, strike-slip and contractional. *In:* Hancock,P.L. (ed.): *Continental deformation.* Pergamon Press, Oxford, 121-142.

Eliassen, H. E., 2003: *Sen-kaledonske og yngre (mesosoiske og kenosoiske) forkastninger på Frøya, Møre-Trøndelag kysten.* Master thesis, University of Bergen, 232pp.

Evans, J. P., Forster, G. B. & Goddard, J. V., 1997: Permeability of fault-related rocks, and implications for hydraulic structure of fault zones. *Journal of Structural Geology 19* (11), 1393-1404.

Fossen, H. & Gabrielsen, R. H., 1996: Experimental modelling of extensional fault systems by use of plaster. *Journal of Structural Geology 18*, 673-687.

Fredman, N., Tveranger, J., Semshaug, S., Braathen, A., & Sverdrup, E., 2007: Sensitivity of fluid flow to fault core architecture and petrophysical properties of fault rocks in siliciclastic reservoirs; a synthetic fault model. *Petroleum Geoscience 13,* 1-16.

Færseth,R.B., Johnsen,E. & Sperrevik,S., 2007: Methodology of risking fault seal capacity: Implications of fault zone architecture. *American Association of Petroleum Geologists 91* (9), 1231-1246.

Gabrielsen, R. H. & Clausen, J. A., 2001: Horses and duplexes in extensional regimes: A scale-modeling contribution. In: Koyi, H. A. & Mancktelow, N. (eds.), Tectonic models: A Volume in Honor of Hans Ramberg. *Geological Society of America Memoir 193,* 219-233.

Gabrielsen,R.H. & Koestler,A.G.,1987: Description and structural

implications of fractures in the late Jurassic sandstones of the Troll Field, northern North Sea. *Norsk Geologisk Tidsskrift 67,* 371-381.

Gabrielsen, R. H., Odinsen, T. & Grunnaleite, I., 1999: Structuring of the Northern Viking Graben and the Møre Basin; the influence of basement structural grain, and the particular role of the Møre-Trøndelag Fault Complex. *Marine and Petroleum Geology 16,* 443-465.

Ghosh, S.K., 1993: *Structural Geology. Fundamentals and Modern Developments.* Pergamon Press, Oxford, 598 pp.

Gibbs, A. D., 1983: Balanced cross-section construction from seismic sections in areas of extensional tectonics. *Journal of Structural Geology 5,* 153-160.

Gibbs, A. D., 1984. Structural evolution of extensional margins. *Journal of the Geological Society of London 141,* 609-620.

Gravesen, P., Rolle, F. & Surlyk, F., 1982: Lithsotratigraphy and sedimentary evolution of the Triassic, Jurassic and Lower Cretaceous of Bornholm. *Danmarks Geologiske Undersøkelse, Serie b. no.7.*

Grønlie, A. & Roberts, D.,1989: Resurgent strike-slip duplex development along the Hitra-Snåsa and Verran Faults, Møre-Trøndelag Fault Zone. *Journal of Structural Geology 11,* 295-305.

Hamann, N.E. 1988: Mesozoikum – Bornholms Geologi I. *Varv 2*, 64-75.

Heynekamp, M. R., Goodwin, L. B., Mozley, P. S. & Haneberg, W. C., 1999: Controls on fault-zone architecture in poorly lithified sediments, Rio Grande rift, New Mexico: implications for fault zone permeability and fluid flow. In: Haneberg, W. C., Mozley, P. S., Moore, J. C. & Goodwin, L. B. (eds.), Faults and subsurface fluid flow. *American Geophysical Union Geophysical Monograph 113,* 27-49.

Kamerling, P., 1979: The geology and hydrocarbon habitat of the Bristol Channel Basin. *Journal of Petroleum Geology, 2* (1), 75-93.

Knipe, R. J., 1997: Juxtaposition and seal diagrams to help analyze fault seals in hydrocarbon reservoirs. *American Association of Petroleum Geologists Bulletin 81,* 187-195.

Knipe, R. J., Fisher, Q. J., Jones, G., Clennell, M. R., Farmer, A. B., Harrison, A., Kidd, B., McAllister, E., Porter, J. R. & White, E. A., 1997: Fault seal analysis: successful methodologies, application and future directions. *In:* Møller-Pedersen, P. & Koestler, A. G. (eds.), Hydrocarbon Seals: Importance for Exploration and Production. *Norwegian Petroleum Society (NPF) Special Publication 7,* 15-40.

Koestler, A. G. & Erhmann, W. U., 1991: Description of brittle extensional features in chalk on the crest of a salt ridge. In: Roberts, A. M. e. a. (eds.), The geometry of normal faults. *Geological Society, London, Special Publication 56,* 113-124.

Liboriussen, J., Ashton, P. & Tygesen, T., 1987: The tectonic evolution of the Fennoscandian Border Zone in Denmark. *Tectonophysics 137,* 21-29.

Lindanger, M. 2003: A study of rock lenses in extensional faults, focusing on factors controlling shapes and dimensions. *Master Thesis, University of Bergen,* xxx pp.

Lindanger, R, Øygaren, M., Gabrielsen, R.H., Mjelde,R., Randen,T. & Tjøstheim, B.A., 2004: Analogue (plaster) modelling and synthetic seismic representation of hangingwall fault blocks above of ramp-flat ramp faults. *First Break 22,* 22-30.

Losh, S., Eglinton, L., Schoell, M. & Woods, J., 1999: Vertical and lateral fluid flow related to a large growth fault, South Eugene Island Block 330 Field, offshore Louisiana. *American Association of Petroleum Geologists Bulletin 83,* 244-276.

Loyd, A. J., Savage, R. J. G., Stride, A. H. & Donovan, D. T., 1973: The geology of the Bristol Channel floor. *Philosophical Transactions of the Royal Society A274,* 595-626.

Manzocchi, T., Walsh, J.J., Nell, P. and Yielding, G. 1999: Fault transmissibility multipliers for flow simulation models. *Petroleum Geoscience 5,* 53-63.

Olsen, E., Gabrielsen, R.H., Braathen, A. & Redfield,T.F., 2007: Fault systems marginal to the Møre Trøndelag Fault Complex, Osen-Vikna area, Central Norway. *Norwegian Journal of Geology 87,* 59-73.

Osmundsen, P.T., Eide, E., Haabesland, N.E, Roberts, D., Andersen, T.B., Kendrick, M., Bingen, B., Braathen, A., & Redfield, T.F., 2006: Kinematics of the Høybakken detachment zone and the Møre-Trøndelag Fault Complex, Central Norway. *Journal of the Geological Society, London 163,* 303-318.

Peacock, D. C. P. & Sanderson, D. J., 1991: Displacements, segment linkage and relay ramps in normal fault zones. *Journal of Structural Geology 13* (6), 721-733.

Peacock, D. C. P. & Sanderson, D. J., 1992: Effects of layering and anisotropy on fault geometry. *Journal of the Geological Society, London 149,* 793-802.

Redfield, T.F., Osmundsen, P.T., Hendriks, B.W.H., 2005: The role of fault reactivation and growth of uplift of western Fennoscandia. *Journal of the Geological Society, London 162,* 1013-1030.

Rykkelid, E. Fossen, H. 2002: Layer rotation around vertical fault overlap zones: observations from seismic data, field examples and physical experiments. *Marine and Petroleum Geology 19,* 181-192.

Shipton, Z. K. & Cowie, P. A., 2003: A conceptual model for the origin of fault damage zone structures in high-porosity sandstone. *Journal of Structural Geology 25,* 333-344.

Shipton, Z.K., Evans, J.P. and Thompson, L.B. 2005: The Geometry and Thickness of Deformation-band Fault Core and its Influence on Sealing Characteristics of Deformation-band Fault Zones. In: Faults, fluid flow and petroleum traps, R. Sorkhabi and Y. Tsuji (eds.), *American Association of Petroleum Geologists Memoir, 85,* pp. 181-195.

Sibson, R. H., 1977: Fault rocks and fault mechanisms. *Geological Society of America Special Paper 303*, 183-203.

Vejbæk, O.V., Stouge, S. & Poulsen, K.D. 1994: Palaeozoic tectonic and sedimentary evolution and hydrocarbon prospectivety in the Bornholm area. Danmarks Geologiske Undersøgelse serie A, 34, 4-2.

Wallace, R.E. and Morris, H.T. 1986: Characteristics of faults and shear zones in deep mines. In: *International structure of fault zones, Birkhaeuser Verlag, Basel, Switzerland 124;* 1-2, 107-125.

Whittaker, A. & Green, G. W., 1983: Geology of the country around Weston-super-Mare, memoir for 1: 50,000 geological sheet 279 New series, with part of sheet 263 and 295. Geological Survey of Great Britain, Institute of Geological Sciences, Her Majesty's Stationary Office, London.

Wojtal, S. F., 1994: Fault scaling laws and the temporal evolution of fault systems. *Journal of Structural Geology 16* (4), 603-612.

Woodcock, N. H. & Schubert, C., 1994: Continental strike-slip tectonics. In: Hancock, P. L. (eds.): *Continental Deformation,* Pergamon Press, 251-263.

Woodward, N. B., Wojtal, S. F., Paul, J. B. & Zadins, Z. Z., 1988: Partitioning of deformation within several external thrust zones of the Appalachians. *Journal of Geology 96,* 351-361.